Unique Rotation Tensor Formulation to Predict Three-Dimensional Deformation Behaviour of Aluminum Alloy AA7010

M. K. Mohd Nor

***Abstract*— The formulation of unique orthogonal rotation tensor $\widehat{\mathbf{R}}$ for rate dependant constitutive model of orthotropic materials is thoroughly discussed in this work. The implementation of this orthogonal rotation tensor is performed by referring to three theorems; the deformation gradient F is invertible, the plastic stretch U is symmetric and positive definite, and finally the rotation tensor $\widehat{\mathbf{R}}$ is assumed orthogonal hence, $\widehat{\mathbf{R}}^{-1} = \widehat{\mathbf{R}}^{T}$. The accuracy and stability of this tensor to define an isoclinic configuration for three-dimensional deformation behaviour of aluminum alloy AA7010 is then demonstrated using Taylor Cylinder Impact test. As adopted in the previous publication, subroutine chkrot93 is used to check the accuracy of the proposed formulation to calculate a proper rotation tensor $\widehat{\mathbf{R}}$. The results proved the accuracy of the proposed rotation tensor and its algorithm to calculate a proper rotation tensor and provide a good agreement with respect to the deformation behaviour of material under consideration.**

***Index Term*— Orthogonal rotation tensor, Orthotropic materials, Three dimensional stress state deformation behaviour**

I. Introduction

IN many engineering components, the orthotropy is induced by a number of manufacturing processes such as rolling and stamping etc. Composites are also examples of orthotropic materials. In fact, most elastoplastic materials exhibit anisotropic behaviour due to their structure orientation and evolution [1]. The constitutive equation based on additive decomposition of generalised strain measures is basically not suitable for the modelling of orthotropic materials' behaviour. As demonstrated in [2], this approach leads to spurious shear stresses which are independent of the elastic material properties for orthotropic materials. Conversely, the multiplicative decomposition of the deformation gradient-based model provides the true behaviour of a constant shear stress [2]. In addition, the evolution of material symmetry in orthotropic materials due to large deformations could not be tracked by the additive strain decomposition based model [3]. Therefore, it can be deduced that this approach is only valid in the case of small strain elasto-plasticity. Strictly speaking, it is restricted for the case where loadings are co-linear with the axis of material orthotropy.

This work is supported by Universiti Tun Hussein Onn Malaysia (UTHM) and Ministry of Higher Education (MOHE) under Fundamental Research Grant Scheme (FRGS) Vot 1547 (Corresponding author to provide e-mail: khir@ uthm.edu.my).

The formulation that is based on the multiplicative decomposition of deformation gradient provides a natural framework for the frame-invariant description of anisotropic elasticity and anisotropic plastic yield [4]. An additive decomposition of strain and strain rate has been found satisfactory for the case of infinitesimal rotations and for uniaxial (non-rotational) deformations [5]. However, such decomposition is not applicable when material is undergoing finite rotations.

This decomposition introduces an intermediate configuration. The plastic intermediate configuration $\bar{\boldsymbol{\Omega}}_p$ is obtained by elastically distressing (unloading) the current configuration $\boldsymbol{\Omega}_t$ to zero stress. This configuration $\bar{\boldsymbol{\Omega}}_p$ differs from the initial configuration $\boldsymbol{\Omega}_0$ by plastic deformation, and differs from the current configuration by elastic deformation. The intermediate configuration in reality does not exist as a continuous map where mappings $\boldsymbol{\Omega}_0 \rightarrow \bar{\boldsymbol{\Omega}}_p$ and $\bar{\boldsymbol{\Omega}}_p \rightarrow \boldsymbol{\Omega}_t$ are not a one-to-one mapping. This is because stress unloading to zero in the actual practice is not physically achievable due to anisotropic hardening and strong Bauschinger effects [6]. Moreover, physically reverse plastic deformation may take place before the stress can be completely unloaded. Therefore the intermediate configuration is conceptually introduced by virtually distressing (reversing) all plastic changes.

One issue related to the multiplicative decomposition is the non-uniqueness of the intermediate configuration. Arbitrary rotations of the local material can be superposed in the intermediate configuration while preserving the unstressed condition. This means the configuration will remains unstressed after being rotated as a rigid body by arbitrary angles. Strictly speaking, the arbitrary rotations give an alternative unstressed configuration, therefore making this configuration non-unique.

To eliminate the non-uniqueness, typically additional requirements dictated by the nature of the considered material model can be adopted [7]. For instance, we may choose the elastic stretch $\mathbf{V}_e$ as the stress response from $\bar{\boldsymbol{\Omega}}_p$ to $\boldsymbol{\Omega}_t$ for elastically isotropic materials. That means elastic rotation tensor $\mathbf{R}_e$ is not involved in the deformation between these configurations. Therefore, the intermediate configuration can be uniquely identified by defining the elastic unloading without rotation.

The intermediate configuration can also be obtained uniquely by defining that the triad of orthogonal vectors attached to the initial configuration remains fixed or unaltered by plastic deformation for orthotropic materials. This

configuration is referred to as isoclinic, and it confirms the uniqueness of the intermediate configuration. Extensive discussion of the non-uniqueness of the multiplicative decomposition can be found in [8] and [9]. This intermediate configuration has been adopted in many constitutive formulations; see for examples [10] and [11]. The chosen of isoclinic configuration makes the proposed formulations in these works compatible with the Mechanical Threshold Stress (MTS) model.

The proposed formulation to define the isoclinic configuration adopted in [11] has been briefly explained in the previous publication [12]. Therefore, this paper is constructed to rigorously discuss the formulation of the proposed orthogonal rotation tensor and further explore the capability to deal with finite strain deformation in three-dimensional mode. The proposed formulation in [11] that is developed in the isoclinic configuration $\bar{\boldsymbol{\Omega}}_i$ provides a unique treatment for elastic and plastic anisotropy. The important features of this constitutive model are the multiplicative decomposition of the deformation gradient $\mathbf{F}$ and a Mandel stress tensor combined with the new stress tensor decomposition generalized for orthotropic materials [13]. The formulation of new Mandel stress tensor $\hat{\boldsymbol{\Sigma}}$ defined in the isoclinic configuration is given by

$$\hat{\boldsymbol{\Sigma}} = \det(\mathbf{F}) \cdot \hat{\mathbf{R}}^T \cdot \left(\mathbf{S} + \frac{\sigma \boldsymbol{\psi}}{\boldsymbol{\psi}\boldsymbol{\psi}} \cdot \boldsymbol{\psi} \right) \cdot \hat{\mathbf{R}}^{-T} \tag{1.1}$$

where $\boldsymbol{\psi}$, $\hat{\mathbf{R}}$, $\boldsymbol{\sigma}$ and $\mathbf{S}$ define the direction of the new volumetric axis in stress space, the orthogonal rotation tensor, the Cauchy stress and the deviatoric stress tensor respectively.

II. ANALYSIS ON THE ROTATION TENSOR $\hat{\mathrm{R}}$

The implementation of the proposed algorithm contained modifications on some subroutines in LLNL-DYNA3D code. Generally speaking, the update of the deviatoric Mandel stress tensor of the new constitutive model proposed in [11] is obtained before been transformed to the current configuration to get the Cauchy stress tensor. Fig. 1 visualises the definition of the isoclinic configuration by using the proposed formulation of the new constitutive model. In this figure, $\mathbf{n}_1$ and $\mathbf{n}_2$ mark the direction of substructure and the continuum, which are identical to each other since the plastic spin $\mathbf{W}_p$ is set to zero.

In DYNA3D code, all constitutive models are given with the Cauchy stress $\boldsymbol{\sigma}$ and the rate of deformation $\mathbf{D}$ tensors at current configuration $\boldsymbol{\Omega}_t$. Therefore, according to the proposed formulation, these tensors must be pulled back to the isoclinic configuration $\bar{\boldsymbol{\Omega}}_i$ by the introduction of orthogonal rotation tensor $\hat{\mathbf{R}}$ before been transformed to the current configuration to get the Cauchy stress tensor at the end of material model subroutine (named f3dm93). Referring to this figure, it can be seen that the application of plastic deformation represented by $\mathbf{U}$ from reference $\boldsymbol{\Omega}_0$ to the isoclinic configurations $\bar{\boldsymbol{\Omega}}_i$ does not change the material orientation but the shape. Equally, the assumption of small elastic deformation adopted in the proposed constitutive model allows changes only in the material orientation from isoclinic $\bar{\boldsymbol{\Omega}}_i$ to the current configurations $\bar{\boldsymbol{\Omega}}_t$ via the rotation tensor $\hat{\mathbf{R}}$. This tensor is used to pull-back the required variables from current $\boldsymbol{\Omega}_t$ to the isoclinic configurations $\bar{\boldsymbol{\Omega}}_i$.

Fig. 1. Isoclinic configuration visualization of M. K. Mohd Nor constitutive model [11]

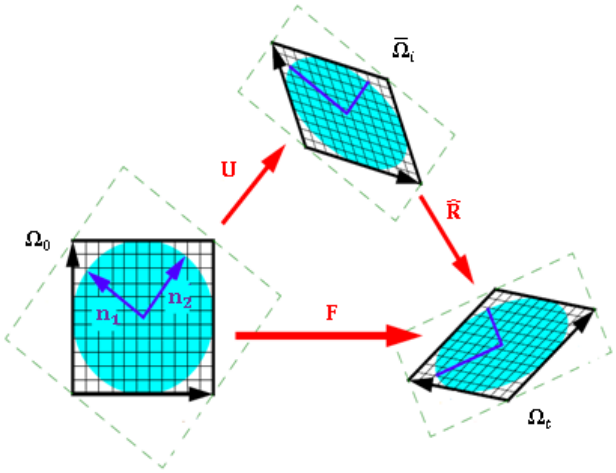

Before starting the implementation of the rotation tensor $\hat{\mathbf{R}}$, a couple of points must be made. First of all, one must bear in mind that the proposed formulation insists on the existence of a unique orthogonal tensor $\hat{\mathbf{R}}$ as well as a unique symmetric positive definite stretch tensor $\mathbf{U}$ for each invertible tensor $\mathbf{F}$. As emphasized in [14], the orthogonal tensor $\hat{\mathbf{R}}$ is considered a proper rotation if, and only if, $\det(\mathbf{F}) > 0$. Based on this discussion, the following theorem is adopted as a reference for a unique rotation tensor $\hat{\mathbf{R}}$ implementation in the subroutine f3dm93 of a newly formulated constitutive model in the LLNL-DYNA3D code named Material Type 93.

- The deformation gradient $\mathbf{F}$ is invertible
- The plastic stretch $\mathbf{U}$ is symmetric and positive definite
- The rotation tensor $\hat{\mathbf{R}}$ is orthogonal hence $\hat{\mathbf{R}}^{-1} = \hat{\mathbf{R}}^T$

III. DIAGONALISATION OF THE PLASTIC STRETCH TENSOR $\mathbf{U}$

Referring to the above theorem, the implementation of the rotation tensor $\hat{\mathbf{R}}$ can be divided into three main stages. Before directly using it, this theorem should first be proved. For this purpose, it is assumed that the tensors $\mathbf{U}$ and $\hat{\mathbf{R}}$ really exist in order to derive an explicit formulation for these tensors by using the deformation gradient $\mathbf{F}$. To prove that the above theorem is acceptable, it requires that the proposed formulation $\mathbf{F} = \mathbf{U} \cdot \hat{\mathbf{R}}$ also exists. Then, the following can be written:

$$\mathbf{F}^T = \mathbf{U}^T \cdot \hat{\mathbf{R}}^T = \mathbf{U} \cdot \hat{\mathbf{R}}^{-1}. \tag{3.1}$$

It can be observed that the properties of symmetric $\mathbf{U}$ and an orthogonal $\hat{\mathbf{R}}$ have been used. In addition, the product of $\mathbf{F}^T \cdot \mathbf{F}$ is always equal to $\mathbf{U}^2$. Accordingly, the stretch $\mathbf{U}$ can be expressed as

$$\mathbf{U} = \mathbf{C}^{1/2} \quad \text{where} \quad \mathbf{C} = \mathbf{F}^T \cdot \mathbf{F} \tag{3.2}$$

The 'helper' tensor $\mathbf{C}$ is assumed positive since

$$\mathbf{a} \cdot \mathbf{C} \cdot \mathbf{a} = \mathbf{a} \cdot \mathbf{F}^T \cdot \mathbf{F} \cdot \mathbf{a} = (\mathbf{F} \cdot \mathbf{a}) \cdot (\mathbf{F} \cdot \mathbf{a}) \tag{3.3}$$

This equation can be written as

$$(\mathbf{F} \cdot \mathbf{a}) \cdot (\mathbf{F} \cdot \mathbf{a}) = \|\mathbf{F} \cdot \mathbf{a}\|^2 > 0 \text{ for all non-zero } \mathbf{a} \tag{3.4}$$

It is noticeable that the magnitude of any vector is never negative. Further, it can be written

$$\|\mathbf{F} \cdot \mathbf{a}\|^2 \geq 0 \tag{3.5}$$

In this case, it is emphasized that the stronger condition is $\|\mathbf{F} \cdot \mathbf{a}\|^2 > 0$. This is satisfied if, and only if, the deformation gradient is invertible; therefore, the product of $\mathbf{F} \cdot \mathbf{a}$ can never be zero for any non-zero vector $\mathbf{a}$. Hence, the possibility of $\|\mathbf{F} \cdot \mathbf{a}\|^2 = 0$ can be ruled out. Note that the 'helper' tensor $\mathbf{C}$ that is used in the above formulation is symmetric, hence diagonal in its principal basis. Furthermore, if the eigenvalues $a_i|i = 1,2,3$ and the eigenvectors $b_i^c|i = 1,2,3$ of tensor $\mathbf{C}$ are known, the following can be written

$$\mathbf{C} = \begin{bmatrix} a_1 & 0 & 0 \\ 0 & a_2 & 0 \\ 0 & 0 & a_3 \end{bmatrix} \tag{3.6}$$

This matrix is defined with respect to the principal $b_i^c|i = 1,2,3$, where the eigenvalues are strictly positive. The basis equation of tensor $\mathbf{C}$ is given by

$$\mathbf{C} = a_1 b_1^c b_1^c + a_2 b_2^c b_2^c + a_3 b_3^c b_3^c \tag{3.7}$$

where the eigenvalues $a_i|i = 1,2,3 > 0$. Great care must be taken to define the square root of tensor $\mathbf{C}$**,** since any positive definite and a symmetric 3x3 matrix in general consist of an infinite number of square roots. A few of them are symmetric but only one can be both symmetric and positive definite [14]. To ensure that a unique $\mathbf{U}$ of Equation (3.2) is obtained, a requirement is set that the square root $\mathbf{C}^{1/2}$ must be a unique positive definite square root, such that

$$\mathbf{U} = d_1 b_1^u b_1^u + d_2 b_2^u b_2^u + d_3 b_3^u b_3^u \tag{3.8}$$

The eigenvalues $d_i|i = 1,2,3$ and the eigenvectors $b_i^u|i = 1,2,3$ of tensor $\mathbf{U}$ can be linked to the eigenvalues $a_i|i = 1,2,3$ and the eigenvectors $b_i^c|i = 1,2,3$ of tensor $\mathbf{C}$ as follows:

$$d_i \equiv +\sqrt{a_i} \quad \text{and} \quad b_3^u = b_3^c \tag{3.9}$$

Further, tensor $\mathbf{U}$ can be written in a matrix form as

$$\mathbf{U} \equiv +\left[\mathbf{C}^{\frac{1}{2}}\right] = \begin{bmatrix} d_1 & 0 & 0 \\ 0 & d_2 & 0 \\ 0 & 0 & d_3 \end{bmatrix} \quad \text{where } d_i \equiv +\sqrt{a_i} \tag{3.10}$$

Consequently, the specific formulation to calculate the square root of matrix $\mathbf{U}$ can be written as

$$\mathbf{U} = [\mathbf{A}] \begin{bmatrix} d_1 & 0 & 0 \\ 0 & d_2 & 0 \\ 0 & 0 & d_3 \end{bmatrix} [\mathbf{A}]^T \quad \text{where} \quad d_i \equiv +\sqrt{a_i} \tag{3.11}$$

As highlighted, the eigenvalues $d_i|i = 1,2,3$ are set to $+\sqrt{a_i}$. In addition, matrix $[\mathbf{A}]$ in Eq. (3.11) contains the eigenvectors of $\mathbf{U}$. This formulation has been adopted in the implementation of the plastic stretch tensor $\mathbf{U}$ of the proposed constitutive model, which is known as the diagonalisation of the matrix square root.

Referring to this formulation, only one square root can be both symmetric and positive definite. Therefore, the formulation of the plastic stretch $\mathbf{U}$ that is defined in Eq. (3.10) is the only stretch that fulfils the given theorem. Accordingly, if the plastic stretch $\mathbf{U}$ exists, then it is proved unique. Once the plastic stretch $\mathbf{U}$ is known, the rotation tensor $\hat{\mathbf{R}}$ eventually can be calculated by

$$\mathbf{U}\hat{\mathbf{R}} = \mathbf{F} \cdot \mathbf{U}^{-1} \tag{3.12}$$

Note that the above equation is a single-valued operation. Therefore, this guarantees the uniqueness of the rotation tensor $\hat{\mathbf{R}}$ due to the uniqueness of the plastic stretch tensor $\mathbf{U}$. The rotation tensor $\hat{\mathbf{R}}$ in fact fulfils the orthogonality requirements of the given theorem. By using Eq. (3.12), the following can be written:

$$\hat{\mathbf{R}}^T \cdot \hat{\mathbf{R}} = \mathbf{U}^{-1} \cdot \mathbf{F}^T \cdot \mathbf{F} \cdot \mathbf{U}^{-1} \tag{3.13}$$

Recalling Eq. (3.2), the above equation can be re-expressed as

$$\mathbf{U}^{-1} \cdot \mathbf{F}^T \cdot \mathbf{F} \cdot \mathbf{U}^{-1} = \mathbf{U}^{-1} \cdot \mathbf{U}^2 \cdot \mathbf{U}^{-1} \tag{3.14}$$

Finally, Eq. (3.14) can be simplified to confirm the orthogonality of the rotation tensor $\hat{\mathbf{R}}$ as follows

$$\mathbf{U}^{-1} \cdot \mathbf{U}^2 \cdot \mathbf{U}^{-1} = \mathbf{U}^{-1} \cdot \mathbf{U} \cdot \mathbf{U} \cdot \mathbf{U}^{-1} = \mathbf{I} \tag{3.15}$$

IV. RENORMALIZATION OF THE ROTATION TENSOR $\hat{\mathrm{R}}$

Based on the discussion in preceding section, the rotation tensor $\hat{\mathbf{R}}$ can be easily calculated by using Eq. (3.15) after the diagonalisation of the plastic stretch tensor $\mathbf{U}$. It is noticed that the given theorem requires that the rotation tensor $\hat{\mathbf{R}}$ is orthogonal. However, the orthogonality of the rotation tensor $\hat{\mathbf{R}}$ is in fact difficult to achieve and maintain in the numerical implementation. It is, therefore, this tensor that should be projected into the space of orthonormal tensors [15]. For this purpose, the methods proposed in [14], have been adopted to perform a renormalization upon the rotation tensor $\hat{\mathbf{R}}$. In two dimensions, the orthogonalisation of the rotation tensor $\hat{\mathbf{R}}$ can be defined explicitly by

$$\hat{\mathbf{R}}_{11} = \left(\hat{\mathbf{R}}_{11} + \hat{\mathbf{R}}_{22}\right)/h$$

$$\begin{aligned}\hat{\mathbf{R}}_{21} &= \left(\hat{\mathbf{R}}_{21} - \hat{\mathbf{R}}_{12}\right)/h \\ \hat{\mathbf{R}}_{12} &= \left(\hat{\mathbf{R}}_{12} - \hat{\mathbf{R}}_{21}\right)/h \\ \hat{\mathbf{R}}_{22} &= \left(\hat{\mathbf{R}}_{11} + \hat{\mathbf{R}}_{22}\right)/h \end{aligned} \tag{4.1}$$

where

$$h = \sqrt{\left(\hat{\mathbf{R}}_{11} + \hat{\mathbf{R}}_{22}\right)^2 + \left(\hat{\mathbf{R}}_{21} - \hat{\mathbf{R}}_{12}\right)^2} \tag{4.2}$$

It can be seen that the above algorithm has fewer operations than the diagonalisation method. In addition, the denominator h of the above algorithm is non-zero for any non-zero determinant matrix. This algorithm is expected to perform well to remap the rotation tensor $\hat{\mathbf{R}}$ (that is arranged in matrix form in DYNA3D) close to the proper orthogonal rotation matrix. Meanwhile, in three dimensions, the orthogonal rotation tensor $\hat{\mathbf{R}}$ is extracted by fixed point iteration. This iteration is set to converge if the maximum stretch of $\hat{\mathbf{R}}$ is less than $\sqrt{3}$. First of all, the rotation tensor $\hat{\mathbf{R}}$ is rescaled as follows:

$$\hat{\mathbf{R}}^0 = \sqrt{\frac{3}{\mathrm{tr}(\hat{\mathbf{R}}^T\hat{\mathbf{R}})}}\hat{\mathbf{R}} \tag{4.3}$$

Supposing that ${g_1}^2 < {g_2}^2 < {g_3}^2$ is the order of the non-zero eigenvalues of $\left(\hat{\mathbf{R}}^0\right)^T\hat{\mathbf{R}}^0$, the construction of ${g_1}^2 + {g_2}^2 + {g_3}^2 = 3$ allows the definition of ${g_3}^2 < 3$. Satisfying this condition, the renormalisation method can be calculated as follows:

$$\hat{\mathbf{R}}_{\text{normalized}} = \frac{1}{2}\hat{\mathbf{R}}\left(3\mathbf{I} - \left(\hat{\mathbf{R}}\right)^T\hat{\mathbf{R}}\right) \tag{4.4}$$

Eq. (4.4) confirms that the 'nearly' orthogonal rotation tensor $\hat{\mathbf{R}}$ is converged and updated to the nearest orthonormal tensor by using the iteration of this algorithm [15].

V. VALIDATION OF THE PROPOSED FORMULATION

The implementation of the rotation tensor $\hat{\mathbf{R}}$ into LLNL-DYNA3D can be found in [12]. Generally, to check and confirm the rotation tensor $\hat{\mathbf{R}}$ that is calculated from the developed algorithm is correct, the subroutine `chkrot93` is called immediately after the renormalization method. It is used to check whether or not a proper rotation tensor $\hat{\mathbf{R}}$ is calculated. The 'proper rotation' tensor $\hat{\mathbf{R}}$ means that the rotation tensor must be orthogonal and the determinant is equal to +1. This subroutine requires only the candidate rotation tensor $\hat{\mathbf{R}}$ in a matrix form as an input, and one value of output is generated then. The output variable is named IERR. In general, there are three different values of output that could possibly be obtained, depending on the examined rotation matrix $\hat{\mathbf{R}}$:

- IERR = 0, if the analysed matrix fulfils the proper rotation requirements.
- IERR = −1, if the analysed matrix is orthogonal but has a negative determinant.
- IERR = ij, if the dot product between column i and column j is wrong.

The output generated is then passed to the subroutine `f3dm93` to ensure that the pull-back transformation upon the related variables from current $\boldsymbol{\Omega}_t$ to the isoclinic $\bar{\boldsymbol{\Omega}}_i$ configurations is correctly performed.

A. Multiple Element Analysis of Cylinder Impact Test

The proposed formulation of orthogonal rotation tensor and the corresponding algorithm has been validated against the uniaxial tensile test of reversed loading and Plate Impact test at 234ms^{-1}, 450ms^{-1} and 895ms^{-1} impact velocities [12]. To ensure the book keeping of the proposed algorithm is efficient to analyse finite strain deformation behaviour of orthotropic materials when impacted with high impact velocity within a three-dimensional stress state, the validation process is further established using multiple elements analysis of a Taylor Cylinder Impact test. A standard configuration of this simulation test is depicted by Figure 2.

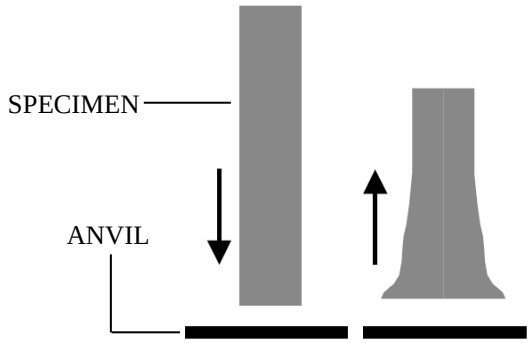

Fig. 2. Diagram of Taylor Cylinder Impact Test

Referring to the above figure, it can be observed that this test creates an impact between a solid cylinder rod of material (specimen) and a fixed rigid surface (anvil) as a target. Strictly speaking, a cylindrical rod is fired into a fixed rigid plate at high velocity (left). This impact subsequently produces permanent deformations in the rebounded cylinder (right**).** The impact at the bottom end of the cylinder happens at a very high strain rate within a three-dimensional stress state and forms a mushroom-shape around the impact area. The higher amplitude of the velocity impact results in a greater mushrooming of the cylinder. Figure 3 shows Finite Element FE model of this test.

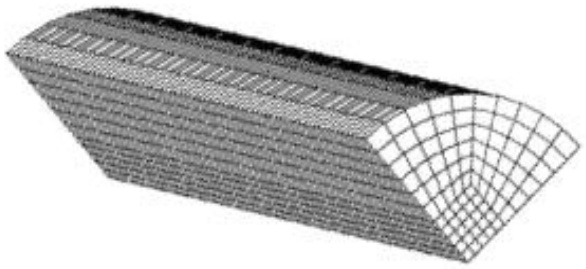

Fig. 3. FE model for Taylor Cylinder Impact Test

In order to reduce the simulation time of this experimental test, the number of elements to model the cylinder is reduced by modelling a quarter of the cylinder with 9.30mm diameter and 46.50mm length. Furthermore, the cylinder is modelled by using a butterfly mesh method with 6375 solid elements, as depicted in this figure. The anvil is modelled as a rigid wall, therefore the impact-interface friction between the solid cylinder rod and the anvil is negligible. The material parameters of aluminum alloy AA7010 are given in Table I.

TABLE I
MATERIAL PROPERTIES OF ALUMINUM ALLOY AA7010

Properties	Value
Young's Modulus	
E_a	70.6 GPa
E_b	71.1 GPa
E_c	70.6 GPa
Poisson's Ratio	
v_{ba}	0.342
v_{ca}	0.342
v_{cb}	0.342
Shear Modulus	
G_{bc}	26.3 GPa
G_{ab}	26.5 GPa
G_{ac}	26.5 GPa
Yield Stress	
σ_y	504 MPa
Tangent Plastic Modulus	
H	0.65 GPa
Hill's Parameters	
R	0.836
P	0.824
Q_{bc}	1
Q_{ba}	1
Q_{ca}	1.0377

VI. RESULTS AND DISCUSSION

Two different impact velocities are used in this analysis: 200ms^{-1} and 214ms^{-1}. The final radius and length of the deformed cylinder profile obtained experimentally are compared with the results generated by proposed formulation. Each case is simulated until 120μs to ensure the final deformed shape of the cylinder profile is really obtained and to ensure the rotation algorithm is consistently calculated throughout the analysis. The deformation behaviour captured at 5μs, 20μs and 50μs is shown in Figure 4.

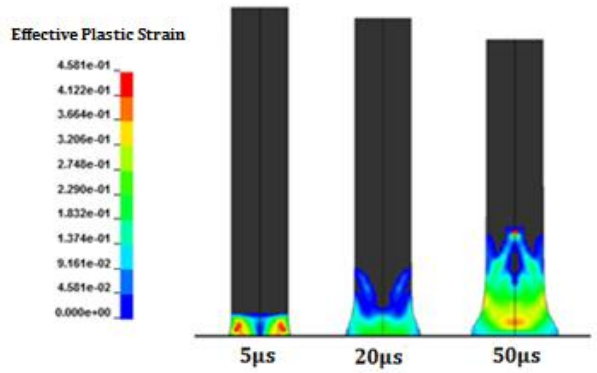

Fig. 4. Deformed mushroom-shape profiles at various instants

The propagation of the elastic compression wave is observable in the simulation test. The effective plastic strain that is raised from the bottom to the top of the cylinders can be seen to have ceased somewhere in the middle of the cylinders hence, no plastic deformation developed at the top of the cylinders. A mushroom-shape is developed in the deformed cylinders near to the impact area. Greater mushrooming is expected for a higher impact velocity.

By using the simulation test data, a radial strain vs. distance from impact end curves of the new material model against the experimental result are plotted in Figure 5 and Figure 6. In these figures, the major and minor side profiles of the deformed cylinder are compared in the case of 200ms^{-1} and 214ms^{-1} impact velocities respectively. Generally, it can be clearly observed that the footprint radius of the deformed cylinder that is impacted with 214ms^{-1} impact velocity is bigger than the footprint radius of the cylinder impacted with 200ms^{-1} impact velocity.

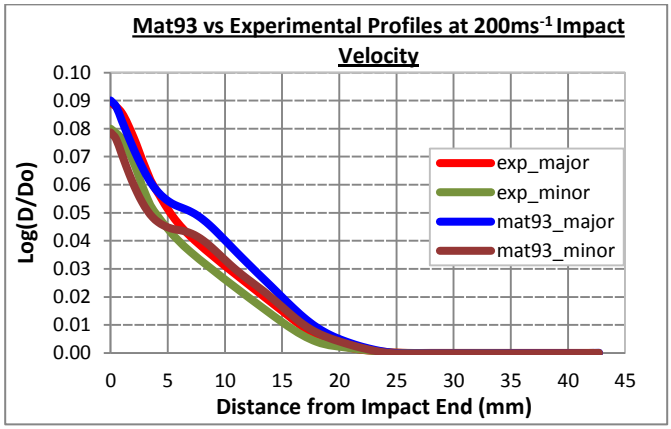

Fig. 5. Major and minor side profile of Taylor Cylinder experimental test results against simulation results

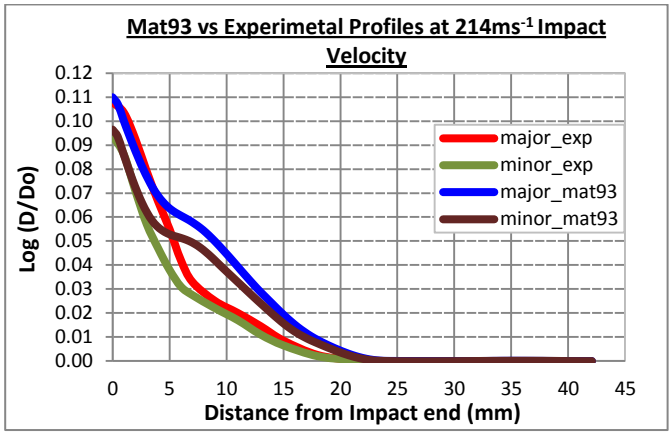

Fig. 6. Major and minor side profile of Taylor Cylinder experimental test results against simulation results

In addition, the final length of the cylinder impacted with a higher impact velocity is smaller than the cylinder impacted with a lower impact velocity. Therefore, an inverse relation between the footprint radius with the shortening of the cylinder length can be established. These criteria are directly influenced by the value of impact velocity. In addition, Figures 5 and 6 show a good agreement with respect to the experimental results in terms of both final footprint radius and length of the deformed cylinder The proposed formulation

however has captured a slightly different mushroom-shape with respect to the experimental results in the case of higher impact velocity ($214ms^{-1}$).

Figure 7 and Figure 8 show the value of IERR calculated by the subroutine `chkrot93` for the corresponding rotation tensor calculated throughout the analysis in both cases. Referring to these figures, it can be concluded that the formulation of the proposed constitutive model has been correctly and successfully integrated in the isoclinic configuration since a proper rotation tensor is obtained throughout the analysis. The results hence established the capability of the proposed formulation of orthogonal rotation tensor to demonstrate three dimensional deformation behaviour of aluminum alloy AA7010.

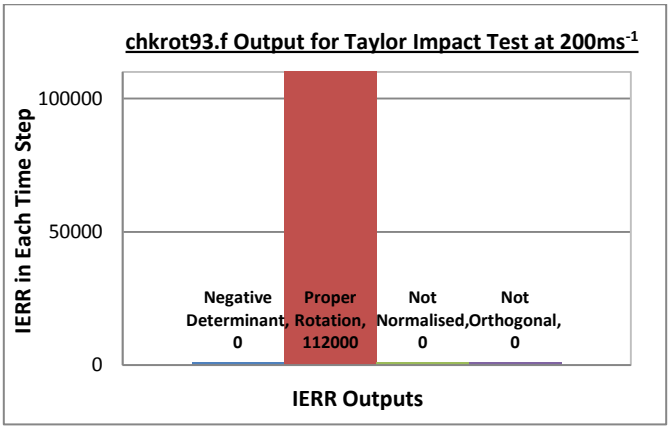

Fig. 7. IERR values at $200ms^{-1}$

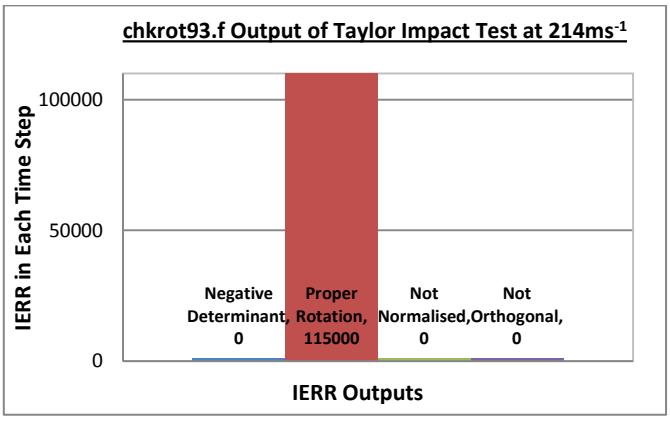

Fig. 8. IERR values at $214ms^{-1}$

VII. CONCLUSION

A new orthogonal rotation tensor is concisely discussed in this paper to correctly define the isoclinic configuration of constitutive model formulated for orthotropic materials. Several theorems are proved and applied to ensure a unique rotation tensor is implemented. The accuracy of the rotation tensor algorithm is examined by the introduction of a new subroutine. The multiple elements analysis of Taylor Cylinder Impact test is used to validate the newly implemented algorithm to deal with three dimensional deformation behaviour of the material under consideration. The results obtained for both impact velocities proved the integration is precisely performed in the isoclinic configuration throughout the analysis using the proposed rotation tensor formulation and capable of providing a satisfactory results to predict finite strain deformation in orthotropic materials. This gives a significant simplification to the numerical implementation of any constitutive equations because one can steer clear of the explicit use of any corotational rate.

ACKNOWLEDGMENT

Author wishes to convey a sincere gratitude to Universiti Tun Hussein Onn Malaysia (UTHM) and Ministry of Higher Education (MOHE) for providing the financial means during the preparation to complete this work under Fundamental Research Grant Scheme (FRGS), Vot 1547.

REFERENCES

[1] Eidel, B., Gruttmann, F. [200] "Elastoplastic Orthotropy at Finite Strains: Multiplicative Formulation and Numerical Implementation," *Computational Materials Science*, 28, 732-742

[2] Itskov, M. [2004] "On the Application of the Additive Decomposition of Generalized Strain Measures in Large Strain Plasticity," *Mech. Res. Commun*. 31, 507-517

[3] Itskov, M. and Aksel, N. [2004] "A constitutive model for orthotropic elasto-plasticity at large strains," *Archive of Applied Mechanics*, 74, 75-91

[4] Belytschko, T., Liu, W. K., Moran, B. [2000] "Nonlinear Finite Elements for Continua and Structures," *John Wiley & Sons Ltd*, Chichester

[5] Reinhardt, W. D. and Dubey, R. N. [1998] "An Eulerian-based Approach to Elastic-plastic Decomposition," *Acta Mechanica*, 131, 111-119

[6] Lubarda, V. A. and Krajcinovic, D. [1995] "Some Fundamental Issues in the Rate Theory of Damage-Elastoplasticity," *Int. J. Plasticity*, 11, 763-797

[7] Lubarda, V.A. [2002] "Elastoplasticity Theory," *CRC Press LLC, Corporate Blvd*., Boca Raton, Florida

[8] Casey, J. and Naghdi, P. [1980] "A Remark on the Use of Decomposition F=FeFp in Plasticity," *Journal of Applied Mechanics*, 47, 672-675

[9] Naghdi, P. [1990] "A Critical Review of the State of Finite Plasticity," *Journal of Applied Mathematics Physics*, 41, 315-394

[10] Vignjevic, R., Djordjevic, N., Panov, V. [2012] "Modelling of Dynamic Behaviour of Orthotropic Metals Including Damage," *Int. J. Plasticity*, 38, 47-85

[11] Mohd Nor, M. K., Vignjevic, R., Campbell, J. [2013a] "Modelling Shockwave Propagation in Orthotropic Materials," *Applied Mechanics and Materials*, Vol. 315, pp 557-561

[12] Mohd Nor, M. K.. [2015] "The Development of Unique Orthogonal Rotation Tensor Algorithm in the LLNL-DYNA3D for Orthotropic Materials Constitutive Model" *Australian Journal of Basic and Applied Sciences*, Vol. 9(37), pp 22-27

[13] Mohd Nor, M. K., Vignjevic, R., Campbell, J. [2013b] "Plane-Stress Analysis of the New Stress Tensor Decomposition," *Applied Mechanics and Materials*, Vol. 315, pp 635-639

[14] Brannon, R. M. [2002] "Rotation: A review of useful theorems involving proper orthogonal matrices referenced to three dimensional physical space," *Computational Physics and Mechanics*, Sandia National Laboratories, Albuquerque

[15] Farnsworth, G. V. and Robinson, A. C. [2003] "Improved Kinematic Options in ALEGRA,' *Sand Report, SAND2003-4510*, Sandia National Laboratories, Albuquerque